

# Sub-10-nm half-pitch electron-beam lithography by using poly(methyl methacrylate) as a negative resist

Huigao Duan<sup>a)</sup>

Department of Electrical Engineering and Computer Science, Massachusetts Institute of Technology, Cambridge, Massachusetts 02139 and School of Physical Science and Technology, Lanzhou University, Lanzhou, Gansu 730000, People's Republic of China

Donald Winston, Joel K. W. Yang,<sup>a)</sup> Bryan M. Cord, Vitor R. Manfrinato, and Karl K. Berggren<sup>b)</sup>

Department of Electrical Engineering and Computer Science, Massachusetts Institute of Technology, Cambridge, Massachusetts 02139

(Received 8 July 2010; accepted 13 September 2010; published 1 December 2010)

Developing high-resolution resists and processes for electron-beam lithography is of great importance for high-density magnetic storage, integrated circuits, and nanoelectronic and nanophotonic devices. Until now, hydrogen silsesquioxane (HSQ) and calixarene were the only two reported negative resists that could approach sub-10-nm half-pitch resolution for electron-beam lithography. Here, the authors report that 10-nm half-pitch dense nanostructures can also be readily fabricated using the well known poly(methyl methacrylate) (PMMA) resist operating in negative tone, even at exposure energies as low as 2 keV. In addition to scanning electron microscopy metrology, transmission electron microscopy metrology was done to confirm the high-resolution capability of negative-tone PMMA. This process was compared to HSQ with salty development and showed similar ultimate resolution, so it could be used as an alternative for applications incompatible with HSQ. © 2010 American Vacuum Society. [DOI: 10.1116/1.3501353]

## I. INTRODUCTION

Ultrahigh-resolution electron-beam lithography (EBL) has promising applications in bit-patterned media for high-density recording,<sup>1</sup> high-resolution and high-accuracy templated self-assembly,<sup>2</sup> nanoelectronic devices,<sup>3</sup> photonic devices,<sup>4</sup> and mask manufacturing for nanoimprint lithography<sup>5</sup> and photolithography. There are many demonstrations of sub-10-nm features patterned in a broad range of resists.<sup>6-9</sup> However, most of the past high resolution features were only realized on sparse structures. Fabrication of dense structures is more challenging than the fabrication of sparse structures due to proximity effect. Many efforts have been made to improve the density of structures by using new tools and new development processes. For example, 12-nm-pitch hydrogen silsesquioxane (HSQ) dot arrays were fabricated by Yang *et al.*<sup>10</sup> using 100 keV exposure combined with high concentration and high temperature development, and 9-nm-pitch HSQ nested “L” structures were fabricated by Yang *et al.*<sup>11</sup> by using a Raith 150<sup>TWO</sup> system at 30 keV combined with high-contrast salty development.<sup>12</sup> However, until now, HSQ and calixarene<sup>13</sup> were the only two reported negative resists that could approach sub-10-nm half-pitch resolution for EBL. Meanwhile, the resolution-limiting factors of electron-beam lithography at the sub-10-nm length scale are not well understood,<sup>11,14</sup> which has limited our ability to further improve its resolution.

Poly(methyl methacrylate) (PMMA) has been used as a high-resolution *positive* electron resist for several decades and sub-10-nm structures have been fabricated by using several special development processes, including low temperature,<sup>6,15,16</sup> megasonic-assisted agitation,<sup>9,16,17</sup> and isopropanol (IPA):water developer.<sup>9,16,17</sup> At the same time, it shows a negative behavior under overexposure,<sup>18,19</sup> and this behavior, due to its simplicity and convenience, has useful applications as masks,<sup>20</sup> mechanical building blocks,<sup>21</sup> and dielectric layers or gaps.<sup>22</sup> In particular, PMMA can also be transformed into carbon or graphitic nanostructures by electron<sup>23,24</sup> or ion beam irradiation,<sup>25</sup> which suggests that, just like many other polymeric resist carbonization processes,<sup>26,27</sup> negative-tone PMMA process could be used to fabricate ultrahigh-resolution patterned carbonaceous nanostructures directly by EBL. However, until now, the highest resolution of all above-mentioned works on negative-tone PMMA was limited at ~15 nm half-pitch<sup>19</sup> and has never been pushed down to sub-10-nm half-pitch.

In this work, we report that sub-10-nm half-pitch dense nanostructures could be fabricated by using PMMA as a negative electron resist. The initial motivation of this work was threefold: (1) developing an additional sub-10-nm-resolution negative resist that could be used as an alternative for applications incompatible with HSQ and calixarene, (2) developing a new high-resolution EBL process that can be used for comparison with existing HSQ processes<sup>11</sup> to understand better the fundamental resolution limits of EBL, and (3) developing a process that could be potentially used for patterning sub-10-nm graphitic structures.

<sup>a)</sup>Present address: Institute of Materials Science and Engineering, Agency for Science, Technology and Research, 3 Research Link, Singapore 117602, Singapore.

<sup>b)</sup>Electronic mail: berggren@mit.edu

## II. EXPERIMENT

PMMA resist (950 K molecular weight, in anisole) from MicroChem Corp. was adopted for exposures. The substrates used were either bulk silicon (100) or 50-nm-thick silicon nitride membrane. After spin-coating, the samples were baked on a hot plate at 180 °C for 60 s to flatten the film, get rid of residual solvent, and enhance the adhesion between PMMA and the substrate. A Raith 150 system was used to conduct all the exposure process with accelerating voltages of 30 or 2 kV and a working distance of  $\sim 6$  mm. Different types of experiments were conducted for different purposes, as described below.

To demonstrate the transformation process of PMMA from positive to negative resist and get the point-spread function of this process, a sparse dot array (15  $\mu\text{m}$  pitch) with the dose range from 3 fC to 3  $\mu\text{C}$  was exposed on 40-nm-thick PMMA on silicon substrate with an aperture size of 20  $\mu\text{m}$  (corresponding to a beam current of  $\sim 180$  pA). After exposure, the sample was developed by 1:2 methyl isobutyl ketone (MIBK):IPA for 60 s at 18 °C. The images were taken on a Raith 150 system with an accelerating voltage of 10 kV and a working distance of  $\sim 6$  mm.

To optimize the development condition and measure the sensitivity, 184-nm-thick PMMA spin-coated on silicon substrate was exposed with the largest beam current  $\sim 4$  nA in the dose range from 300 to 24  $\text{mC}/\text{cm}^2$ . The pattern for this purpose was a series of  $20 \times 60 \mu\text{m}^2$  bars. After exposure, the samples were developed in different developers (including acetone, N-methylpyrrolidone, MIBK, MIBK:IPA, and chlorobenzene) with different temperatures (from 18 to 54 °C) and different development times (from 30 s to 10 min). After development, the height of the bars on the developed samples was measured by a profilometer (KLA Tencor P16). Sensitivity values were defined as the dose  $D_s$  necessary to achieve 50% of its maximum thickness after development. Contrast values were determined by  $\gamma = 0.75/\lg(D_{0.75}/D_0)$ , where  $D_{0.75}$  was the area dose at 75% of the maximum remaining thickness and  $D_0$  was the area dose at the onset of incomplete development. According to the measurements, MIBK was determined to be the best developer when operated at 30 °C, while development time had no detectable effect on the contrast by using MIBK developer. It should be noted here that MIBK can only remove exposed low-molecular PMMA and is not a good remover for completely unexposed PMMA, so it cannot be used to develop sparse structures to obtain complete negative-tone features. In our experiments, the features were very dense, so the PMMA between designed features could be exposed by parasitic electron dose due to proximity effect.

To get high-resolution structures, 22-nm-thick PMMA was exposed on silicon substrate with a smaller beam spot size by adopting the aperture size of 20  $\mu\text{m}$ . After exposure, the sample was developed by MIBK at 30 °C for 2 min and rinsed by IPA for 1 min. Before imaging, a Au/Pd layer was deposited on the surface. The images were also taken by

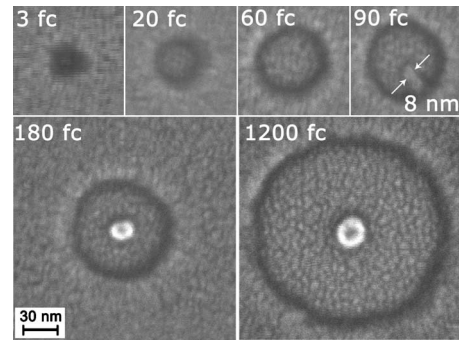


FIG. 1. SEM images showing the resulting structures in developed PMMA as a function of point exposure dose in electron-beam lithography. PMMA was 40 nm thick and exposure was done at 30 kV with a beam current  $\sim 400$  pA. PMMA was subsequently developed by 1: 2 MIBK: IPA at 18 °C for 60 s. The sub-10-nm cross-linked PMMA feature was exposed at a dose of 90 fC/dot.

using a Raith 150 electron microscope/lithography system with an accelerating voltage of 10 kV and a working distance of  $\sim 6$  mm.

To determine the quality of fabricated structures and confirm the high-resolution capability of negative-tone PMMA, a thinner PMMA (16 nm) was used and high-resolution lithography was performed on both silicon substrate and 50-nm-thick silicon nitride membrane substrate (Ted Pella Corp.). All other parameters were the same as those in the previous high-resolution experiment. The fabricated structures on silicon were measured by SEM and those on silicon nitride were measured by using a JEOL JEM 2010F high-resolution transmission electron microscope operated on 200 kV in bright field mode.

Finally, to study the possibility of improving the sensitivity of negative-tone PMMA process while keeping its high-resolution capability, we exposed PMMA at different energies of 30, 20, 10, 5, and 2 keV. We measured the on-set dose of an isolated dot to determine the sensitivity at different voltages and did high-resolution electron-beam lithography at 2 keV. The development process was the same as that in 30-keV exposure.

## III. RESULTS AND DISCUSSION

In this section, we will present and discuss the results of our experiments on point-spread function, development contrast, sensitivity, and resolution limit of negative-tone PMMA process.

### A. Point-spread function

Figure 1 gives the typical evolution of PMMA resist when increasing the dot dose, which shows the transformation process of PMMA from a positive to a negative resist. From this figure, we know that the onset dose of negative-tone PMMA was about 30 times higher than positive-tone PMMA. We believe the transformation was a carbonization process.<sup>28</sup> Through measuring the diameters of both negative and positive structures at different doses, we can obtain their point-spread functions (PSFs), as shown in Fig. 2, which was de-

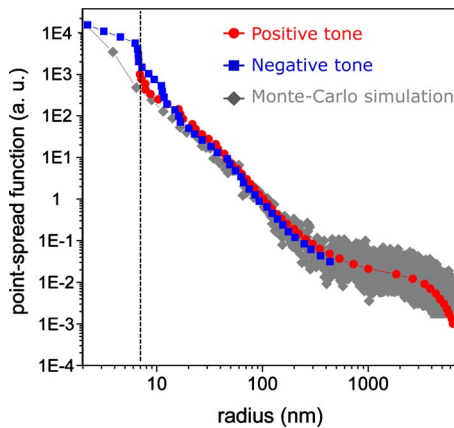


FIG. 2. (Color online) Experimentally measured PSFs of positive-tone (dot) and negative-tone (square), and Monte Carlo simulated PSF (rhombus) at 30 kV with a 3 nm spot size on 40-nm-thick PMMA. The left of the dashed line is the metrology-limited region.

terminated by plotting  $1/\text{dose}$  versus the measured feature radius.<sup>29</sup> By comparing the PSFs of positive-tone PMMA, negative-tone PMMA, and Monte Carlo simulation (home-made program, based on the codes in Ref. 30, and the simulation parameters were 30 kV, 3 nm spot size, silicon substrate, 40 nm PMMA, 50 000 electrons, and including secondary electrons), we can see that they have very similar PSF profiles when the range is larger than 7 nm, which means different kinds of electrons, such as backscattered electrons or backscattered-electron-induced-secondary-electrons, played very similar roles in the scission and cross-linking of positive- and negative-tone PMMA, respectively. Thus, the only difference between positive- and negative-tone PMMA was their sensitivity. The PSF of negative-tone PMMA in the range  $<7$  nm was different from simulation, which was probably induced by the limitation of the PSF measurement method, including both the metrology and the extraction model.

## B. Development contrast and sensitivity

Figure 3 shows the contrast curve using MIBK as the developer at 30 °C for 2 min, from which we can obtain the contrast value  $\sim 4$  and sensitivity  $\sim 5.8$  mC/cm<sup>2</sup>. The contrast value is not high relative to high-resolution development processes for positive-tone PMMA (such as low temperature development<sup>6</sup>) and HSQ (such as salty development<sup>12</sup> and high temperature and high concentration TMAH development<sup>10</sup>). The sensitivity of negative-tone PMMA is about 30 times lower than positive-tone PMMA and is similar to other high-resolution negative resists such as calixarene,<sup>7</sup> fullerene-based film,<sup>31</sup> and ZnO.<sup>32</sup> However, the sensitivity of PMMA can be dramatically improved by adopting lower-voltage exposure (see Sec. III D) and lower temperature development.<sup>6</sup>

## C. Resolution limit at 30 keV

Figures 4(a) and 4(b) show the 10-nm-half-pitch nested L's and the hexagonally close-packed dots, respectively.

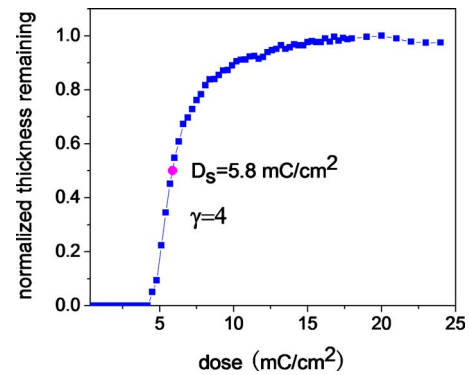


FIG. 3. (Color online) Plot of normalized thickness remaining of PMMA film as a function of dose using MIBK as the developer at 30 °C for 2 min. The contrast value  $\gamma$  and sensitivity  $D_s$  were  $\sim 4$  and 5.8 mC/cm<sup>2</sup>, respectively. It should be noted that the minimum area dose we used in the exposure was 300  $\mu\text{C}/\text{cm}^2$ , so the positive-tone behavior of PMMA was not shown in this figure.

can be seen that 10-nm half-pitch can be clearly resolved. As shown in Figs. 4(c) and 4(d), patterns down to 6-nm half-pitch for dense lines and 8-nm half-pitch for dense dots still showed some response. However, the high aspect ratio of the structures caused feature collapse and led to difficulties in metrology for these patterns. A very thin Au/Pd layer ( $\sim 1$  nm) was deposited on the surface to increase the image contrast, which was necessary due to the low secondary electron yield of the carbonaceous system. However, the Au/Pd layer also prevented us from getting more accurate measurements because the grain size was on the same scale as our structures.

Figure 5 shows both SEM images and TEM micrographs of the nested L's using 16-nm-thick PMMA as the resist, where 1:3 line-space patterns on a 20 nm pitch were fabri-

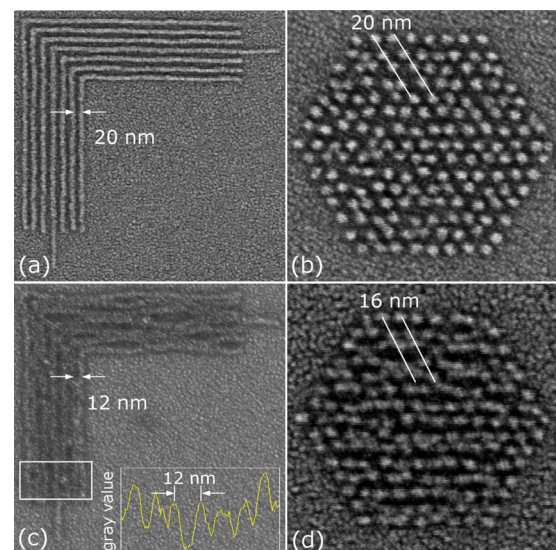


FIG. 4. (Color online) SEM images of ultrahigh-resolution structures fabricated by the Raith 150 system at MIT at 30 kV using 22-nm-thick PMMA as a negative resist. [(a) and (b)] 20-nm-pitch nested “L” structures and hexagonally close-packed dots, (c) 12-nm-pitch nested L's, and (d) 16-nm-pitch hexagonally close-packed dots.

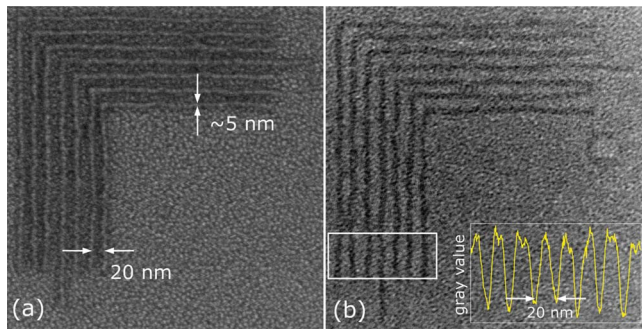


FIG. 5. (Color online) (a) SEM and (b) bright field TEM images of 20-nm-pitch negative-tone PMMA nested L's, showing 5 nm lines were fabricated with a 15 nm space. The thickness of PMMA here was 16 nm. TEM image was taken with a slight underfocus to enhance the image contrast. The structures for TEM metrology was fabricated on 50-nm-thick freestanding SiN membrane.

cated. Compared with the high-contrast HSQ process in the same equipment, negative-tone PMMA had almost the same resolution limit of  $\sim 12$  nm pitch<sup>12</sup> without using a special development process (i.e., much lower development contrast), which suggests that the development contrast value was not vital for high-density electron-beam lithography in this case.

#### D. Low-voltage exposure

Low-voltage exposure was not attractive in the past due to its low resolution and low penetrating depth. Its highest reported resolution at sub-5 keV was 50 nm pitch using calixarene as a resist.<sup>33</sup> However, its exposure sensitivity is much higher compared to high voltage.<sup>34</sup> Figure 6 shows the onset dose as a function of accelerating voltage, which was measured by using a single negative-tone PMMA dot as the test pattern. From Fig. 6, we can see that the sensitivity increased almost linearly with decreasing accelerating voltage.

For large-volume applications of electron-beam lithography, exposure time and cost have become the bottlenecks; thus, low-voltage exposure has been considered as an option

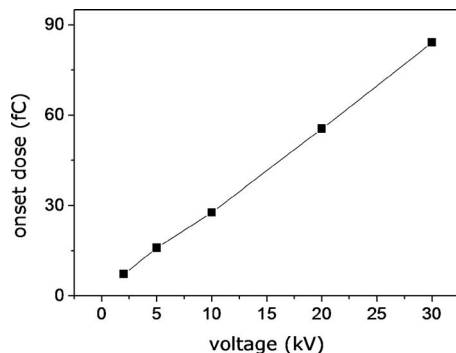


FIG. 6. Onset dose of a negative-tone PMMA dot as a function of voltage. The thickness of PMMA was 40 nm, and the beam current for 30, 20, 10, 5, and 2 kV were 372, 346, 227, 174, and 126 pA, respectively. It should be noted that the difference of beam current of different voltages is dependent on the electron column design, so we did not use exposure time as the indicator for efficiency.

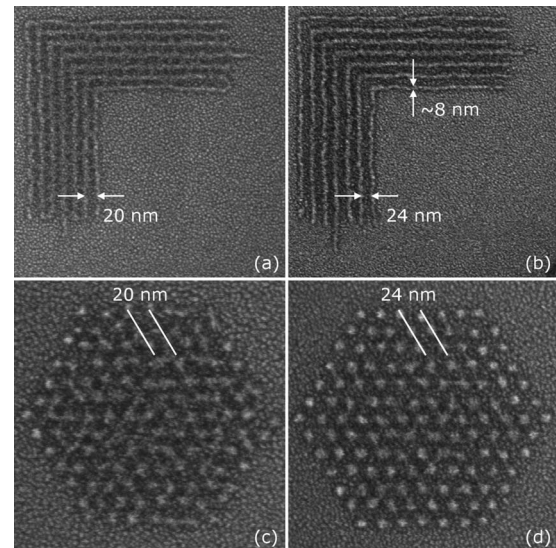


FIG. 7. SEM images of (a) 20-nm-pitch nested L's, (b) 24-nm-pitch nested L's, (c) 20-nm-pitch hexagonally close-packed dots, and (d) 24-nm-pitch hexagonally close-packed dots, fabricated by the Raith 150 system at MIT at 2 keV using 16-nm-thick PMMA as a negative resist. During exposure, the aperture size was set to 10  $\mu\text{m}$  and the corresponding beam current was  $\sim 20$  pA and work distance was  $\sim 6$  mm. The electron doses were [(a) and (b)] 2 nC/cm, (c) 3 fC/dot, and (d) 4 fC/dot. The sample was developed in 1:2 MIBK:IPA for 1 min.

because of its high sensitivity and low cost. MAPPER has developed a multibeam system equipped with a 5 kV electron column and there are plans to adopt it for integrated circuit manufacturing, which is competitive with EUV.<sup>35</sup> Very recently, Manfrinato *et al.*<sup>36</sup> pushed the resolution to 20 nm pitch at 2 keV by using HSQ as a resist. In our exposure, by using PMMA as a negative resist, sub-10-nm features were also fabricated, 10-nm half-pitch was resolvable, and 12-nm half-pitch was clearly resolved, as shown in Fig. 7. These results indicate that sub-10-nm structures can also be fabricated efficiently by using negative-tone PMMA.

#### IV. CONCLUSION

The central result of this article demonstrated the use of PMMA as a negative resist for ultrahigh-resolution electron-beam lithography. By using MIBK as the developer, 10-nm half-pitch dense nanostructures were fabricated and 6-nm half-pitch still showed response. TEM metrology indicates a good quality of the fabricated sub-10-nm structures, and low-voltage exposure showed that the high-resolution sub-10-nm structures can be also fabricated with a reasonable sensitivity. Considering PMMA itself is a polymer while overexposed PMMA is a carbonaceous material, high-resolution electron-beam lithography using PMMA as a negative resist has promising potential applications in carbon-based nanoscience and nanotechnology. In addition, by choosing proper pattern design and development parameters, PMMA could be used as both positive and negative resists to produce exotic structures. However, before adopting this process for applications, much work should be done to study the mechanism

of this process, improve the image contrast, transfer the pattern to functional layers, and study the physical properties of negative-tone PMMA for applications.

## ACKNOWLEDGMENTS

The authors thank Henry I. Smith, James M. Daley, and Mark K. Mondol for helpful discussions and Juan Ferrera for providing PSF Monte Carlo Simulation codes. Electron-beam lithography was done in MIT's shared scanning-electron-beam-lithography facility in the Research Laboratory of Electronics. H.D. would like to acknowledge his part fellowship from China Scholarship Council, and Erqing Xie and Li Han for their suggestions on experiments. V.R.M. was supported by the Excitonics Frontier Research Center at MIT in this research. This work was funded by the Information Storage Industry Consortium, Nanoelectronics Research Initiative, and King Abdulaziz City for Science and Technology.

- <sup>1</sup>B. D. Terris and T. Thomson, *J. Phys. D* **38**, R199 (2005).
- <sup>2</sup>I. Bitá, J. K. W. Yang, Y. S. Jung, C. A. Ross, E. L. Thomas, and Karl K. Berggren, *Science* **321**, 939 (2008).
- <sup>3</sup>Z. Chen, Y.-M. Lin, M. J. Rooks, and P. Avouris, *Physica E (Amsterdam)* **40**, 228 (2007).
- <sup>4</sup>J. K. W. Yang, A. J. Kerman, E. A. Dauler, B. Cord, V. Anant, R. J. Molnar, and K. K. Berggren, *IEEE Trans. Appl. Supercond.* **19**, 318 (2009).
- <sup>5</sup>W. Wu *et al.*, *Nano Lett.* **8**, 3865 (2008).
- <sup>6</sup>B. Cord, J. Lutkenhaus, and K. K. Berggren, *J. Vac. Sci. Technol. B* **25**, 2013 (2007).
- <sup>7</sup>J. Fujita, Y. Ohnishi, Y. Ochiai, and S. Matsui, *Appl. Phys. Lett.* **68**, 1297 (1996).
- <sup>8</sup>M. S. M. Saifullah, K. R. V. Subramanian, E. Tapley, D.-J. Kang, M. E. Welland, and M. Butler, *Nano Lett.* **3**, 1587 (2003).
- <sup>9</sup>S. Yasin, D. G. Hasko, and H. Ahmed, *Appl. Phys. Lett.* **78**, 2760 (2001).
- <sup>10</sup>X. M. Yang, S. Xiao, W. Wu, Y. Xu, K. Mountfield, R. Rottmayer, K. Lee, D. Kuo, and D. Weller, *J. Vac. Sci. Technol. B* **25**, 2202 (2007).
- <sup>11</sup>J. K. W. Yang, B. Cord, H. G. Duan, K. K. Berggren, J. Klingfus, S. W. Nam, K. B. Kim, and M. J. Rooks, *J. Vac. Sci. Technol. B* **27**, 2622 (2009).
- <sup>12</sup>J. K. W. Yang and K. K. Berggren, *J. Vac. Sci. Technol. B* **25**, 2025 (2007).
- <sup>13</sup>Zulfakri bin Mohamad, Masumi Shirai, Hayato Sone, Sumio Hosaka, and Masatoshi Kodera, *Nanotechnology* **19**, 025301 (2008).
- <sup>14</sup>B. Cord, J. K. W. Yang, H. Duan, D. C. Joy, J. Klingfus, and K. K. Berggren, *J. Vac. Sci. Technol. B* **27**, 2616 (2009).
- <sup>15</sup>W. Hu, K. Sarveswaran, M. Lieberman, and G. H. Bernstein, *J. Vac. Sci. Technol. B* **22**, 1711 (2004).
- <sup>16</sup>M. J. Rooks, E. Kratschmer, R. Viswanathan, J. Katine, R. E. Fontana, and S. A. MacDonald, *J. Vac. Sci. Technol. B* **20**, 2937 (2002).
- <sup>17</sup>W. Chen and H. Ahmed, *Appl. Phys. Lett.* **62**, 1499 (1993).
- <sup>18</sup>I. Zailer, J. E. F. Frost, V. Chabasseur-Molyneux, C. J. B. Ford, and M. Pepper, *Semicond. Sci. Technol.* **11**, 1235 (1996).
- <sup>19</sup>A. C. F. Hoole, M. E. Welland, and A. N. Broers, *Semicond. Sci. Technol.* **12**, 1166 (1997).
- <sup>20</sup>S. Wang, D. F. P. Pile, C. Sun, and X. Zhang, *Nano Lett.* **7**, 1076 (2007).
- <sup>21</sup>W. H. Teh and C. G. Smith, *J. Vac. Sci. Technol. B* **21**, 3007 (2003).
- <sup>22</sup>W. H. Teh, C.-T. Liang, M. Graham, and C. G. Smith, *J. Microelectromech. Syst.* **12**, 641 (2003).
- <sup>23</sup>H. Duan, E. Xie, L. Han, and Z. Xu, *Adv. Mater.* **20**, 3284 (2008).
- <sup>24</sup>H. G. Duan, E. Q. Xie, and L. Han, *J. Appl. Phys.* **103**, 046105 (2008).
- <sup>25</sup>Y. Koval, *J. Vac. Sci. Technol. B* **22**, 843 (2004).
- <sup>26</sup>J. A. Lee, K.-C. Lee, S. I. Park, and S. S. Lee, *Nanotechnology* **19**, 215302 (2008).
- <sup>27</sup>R. Du, S. Ssenyange, M. Aktary, and M. T. McDermott, *Small* **5**, 1162 (2009).
- <sup>28</sup>H. Duan, J. Zhao, Y. Zhang, E. Xie, and L. Han, *Nanotechnology* **20**, 135306 (2009).
- <sup>29</sup>R. Menon, D. Gil, and H. I. Smith, *J. Opt. Soc. Am. A* **23**, 567 (2006).
- <sup>30</sup>R. A. Ghanbari, Ph.D. thesis, Massachusetts Institute of Technology, 1993.
- <sup>31</sup>F. P. Gibbons, M. Manickam, J. A. Preece, R. E. Palmer, and A. P. G. Robinson, *Small* **5**, 2750 (2009).
- <sup>32</sup>M. S. M. Saifullah, K. R. V. Subramanian, D.-J. Kang, D. Anderson, W. T. S. Huck, G. A. C. Jones, and M. E. Welland, *Adv. Mater.* **17**, 1757 (2005).
- <sup>33</sup>M. Peuker, *Microelectron. Eng.* **53**, 337 (2000).
- <sup>34</sup>A. Tilke, M. Vogel, F. Simmel, A. Kriele, R. H. Blick, H. Lorenz, D. A. Wharam, and J. P. Kotthaus, *J. Vac. Sci. Technol. B* **17**, 1594 (1999).
- <sup>35</sup>J. J. H. Chen, S. J. Lin, T. Y. Fang, S. M. Chang, F. Krecinic, and B. J. Lin, *International Symposium on VLSI Technology, Systems, and Applications, VLSI-TSA '09 (IEEE, Hsinchu, Taiwan, 2009)*, pp. 96–97.
- <sup>36</sup>V. R. Manfrinato, L. L. Cheong, H. G. Duan, D. Winston, H. I. Smith, and K. K. Berggren, *J. Vac. Sci. Technol. B* (submitted).